

Soliton states in mesoscopic two-band-superconducting cylinders

S.V. Kuplevakhsy, A.N. Omelyanchouk, and Y.S. Yerin

*B. Verkin Institute for Low Temperature Physics and Engineering of the National Academy of Sciences of Ukraine
47 Lenin Ave., Kharkov 61103, Ukraine
E-mail: kuplevakhsy@ilt.kharkov.ua*

Received February 16, 2011

In the framework of the Ginzburg-Landau approach, we present a self-consistent theory of specific soliton states in mesoscopic (thin-walled) two-band-superconducting cylinders in external parallel magnetic fields. Such states arise in the presence of "Josephson-type" interband coupling, when phase winding numbers are different for each component of the superconducting order parameter. We evaluate the Gibbs free energy of the system up to second-order terms in a certain dimensionless parameter $\varepsilon \approx \mathcal{L}_m/\mathcal{L}_k \ll 1$, where \mathcal{L}_m and \mathcal{L}_k are the magnetic and kinetic inductance, respectively. We derive the complete set of exact soliton solutions. These solutions are thoroughly analyzed from the viewpoint of both local and global (thermodynamic) stability. In particular, we show that rotational-symmetry-breaking caused by the formation of solitons gives rise to a zero-frequency rotational mode. Although soliton states prove to be thermodynamically metastable, the minimal energy gap between the lowest-lying single-soliton states and thermodynamically stable zero-soliton states can be much smaller than the magnetic Gibbs free energy of the latter states, provided that intraband "penetration depths" differ substantially and interband coupling is weak. The results of our investigation may apply to a wide class of mesoscopic doubly-connected structures exhibiting two-band superconductivity.

PACS: 05.45.Yv Solitons;
74.20.De Phenomenological theories.

Keywords: two-band superconductor, soliton state.

1. Introduction

The subject of this paper is a self-consistent theory of specific soliton states that were originally predicted in Ref. 1 and reportedly observed experimentally [2]. Without any doubt, these states can be regarded as a hallmark of two-band superconductivity in mesoscopic doubly-connected samples.

Indeed, owing to the emergence of additional degrees of freedom of the order parameter, the nomenclature of topological objects in multiband superconductors is much richer than that in conventional single-band superconductors. In particular, Ginzburg-Landau equations describing two-band superconductivity in bulk samples admit topologically stable solutions (with one-dimensional singularities of the order parameter) that can be interpreted as vortices carrying fractional magnetic flux [3]. In the absence of any interband coupling, these vortices are accompanied by a circulating neutral superflow associated with gradients of the interband phase difference. In the presence of "Josephson-type" interband coupling, the neutral superflow generates static solitons of the sine-Gordon type. In contrast to traditional Abri-

kov vortices in type-II superconductors, the energy per unit length of these composite topological defects diverges at spatial infinity: hence they are thermodynamically metastable and difficult to create in bulk samples.

However, solitons of the interband phase difference can exist by themselves in doubly-connected mesoscopic samples, when the formation of any magnetic vortices in the volume of the superconductor is prohibited energetically [1]. Moreover, soliton states in this case can be induced by an externally applied magnetic field, which makes them a convenient object of investigation. Thus, experimental studies [2] of the magnetic response of mesoscopic two-band superconducting rings reveal certain nontrivial features that, according to the authors of Ref. 2, can be attributed to the creation of metastable soliton states.

Our research is largely motivated by the absence in current literature of any quantitative theoretical analysis of this pronounced feature of two-band superconductivity. (Unfortunately, the arguments of Ref. 1 and of the recent publications [4] are mostly heuristic by nature.) Mathematically, the approach of this paper is based on a Ginzburg-

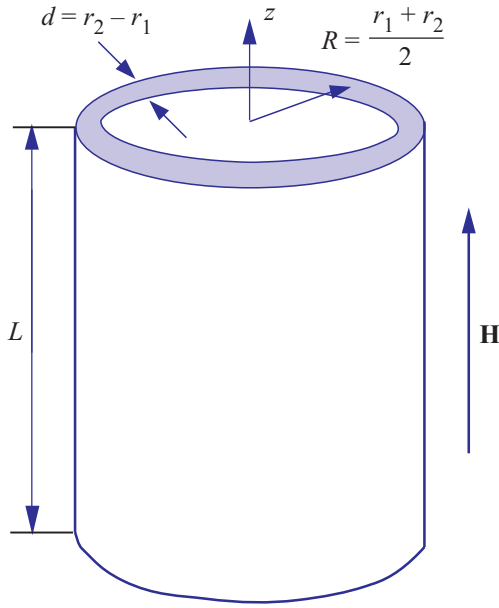


Fig. 1. The geometry of the problem (schematically). The parameters L , R and d obey conditions (2)–(5).

Landau-type theory, which is a commonplace in theoretical studies of topological defects in two-band superconductors: see the next section. This means, of course, that we are restricted to the temperature range

$$\frac{T_c - T}{T_c} \ll 1,$$

where T_c is the critical temperature of the superconducting transition.

As to the physical object, we consider a two-band superconductor in the form of a straight, circular thin-walled cylinder, whose symmetry axis is the z axis of cylindrical coordinates (r, φ, z) (see Fig. 1). The constant external magnetic field \mathbf{H} is applied along the symmetry axis: $\mathbf{H} = (0, 0, H > 0)$. The length of the generatrix of the wall of the cylinder satisfies the condition

$$L \gg R \equiv \frac{r_1 + r_2}{2}, \quad (1)$$

which allows us to neglect end effects. The wall thickness $d \equiv r_2 - r_1$ and the average radius of the cylinder R satisfy the following conditions:

$$d \ll \min\{\xi_1, \xi_2\}, \quad (2)$$

$$R \gg \max\{\xi_1, \xi_2\}, \quad (3)$$

$$R \gg \lambda, \quad (4)$$

$$\varepsilon \equiv \frac{dR}{2\lambda^2} \ll 1, \quad (5)$$

where ξ_1 and ξ_2 are the "coherence lengths" in bands 1 and 2, respectively, and λ is the weak-field penetration depth.

Exact definitions of ξ_1 , ξ_2 , and λ will be given in the next section; however, the role of conditions (2)–(5) should be explained right now. Thus, condition (2) precludes the formation of any magnetic vortices in the wall of the cylinder. Condition (3) mainly simplifies mathematical consideration. In contrast, a combination of conditions (4) and (5) is of primary importance: taken together, these two conditions guarantee that self-induced magnetic fields are small and can be treated perturbatively. (This fact justifies the definition "mesoscopic cylinders" in the title of the paper.) Moreover, as will be shown, the dimensionless quantity ε serves as a natural expansion parameter of the Gibbs free energy. In order to carry out a rigorous analysis of thermodynamic stability of soliton states, we will have to evaluate the Gibbs free energy exactly up to small terms of order ε^2 , which implies the necessity of self-consistent evaluation of the vector potential up to first-order terms in ε .

We conclude the formulation of the problem by specifying boundary conditions for soliton states. Consider a two-component superconducting order parameter $\Psi = (\psi_1, \psi_2)$ where $\psi_1 = |\psi_1|e^{i\phi_1}$ and $\psi_2 = |\psi_2|e^{i\phi_2}$. The double-connectedness of the cylinder is accounted for by the condition of single-valuedness of Ψ . [5] In particular, this condition requires that

$$|\psi_1|_{\varphi=0} = |\psi_1|_{\varphi=2\pi}, \quad |\psi_2|_{\varphi=0} = |\psi_2|_{\varphi=2\pi}. \quad (6)$$

As to the phases ϕ_1 and ϕ_2 , the requirement is as follows:

$$\oint_{\Gamma} \nabla \phi_1 \cdot d\mathbf{l} = 2\pi n_1, \quad \oint_{\Gamma} \nabla \phi_2 \cdot d\mathbf{l} = 2\pi n_2, \quad n_{1,2} = 0, \pm 1, \pm 2, \dots, \quad (7)$$

where Γ is an arbitrary closed continuous contour that lies inside the wall of the cylinder and encircles the opening. It should be emphasized that there are no a priori reasons for setting $n_1 = n_2$ [6]. As in the case of fractional magnetic vortices in bulk two-band superconductors [3], nontrivial topological states arise when $n_1 \neq n_2$. In the presence of interband coupling, they are of the soliton type.

In Sec. 2, we introduce the Gibbs free-energy functional of the system and analyze its basic properties. In Sec. 3, we derive a self-consistent expression for the electromagnetic Gibbs free energy. Soliton solutions are derived and thoroughly discussed in Sec. 4. Finally, in Sec. 5, we summarize the obtained results and make several concluding remarks. Appendices 1 and 2 contain details of some mathematical calculations skipped over in the main text. In Appendix 3, we present several particular examples of soliton solutions.

2. Gibbs free-energy functional

We begin by defining the Gibbs free-energy functional of the system. In view of complete homogeneity along the z axis and with the normal-state Gibbs free energy being subtracted, it takes the following form:

$$G[\Psi, \Psi^*, \mathbf{A}; \mathbf{H}] = L \int_{\Sigma_S} d^2\mathbf{r} \left[\alpha_1 |\psi_1|^2 + \alpha_2 |\psi_2|^2 + \frac{\beta_1}{2} |\psi_1|^4 + \frac{\beta_2}{2} |\psi_2|^4 + \frac{1}{2m_1} \left| \left(-i\hbar\nabla - \frac{2e}{c} \mathbf{A} \right) \psi_1 \right|^2 + \frac{1}{2m_2} \left| \left(-i\hbar\nabla - \frac{2e}{c} \mathbf{A} \right) \psi_2 \right|^2 - \gamma (\psi_1 \psi_2^* + \psi_1^* \psi_2) \right] + \frac{L}{8\pi} \int_{\Sigma_S + \Sigma_O} d^2\mathbf{r} (\mathbf{h} - \mathbf{H})^2. \quad (8)$$

Here, the coefficients β_1 and β_2 are positive constants, whereas α_1 and α_2 are temperature-dependent:

$$\alpha_1 = \alpha_1(T) \equiv a_1(T - T_1), \quad \alpha_2 = \alpha_2(T) \equiv a_2(T - T_2), \quad (9)$$

$$a_1, a_2, T_1, T_2 > 0.$$

Moreover, the latter coefficients enter the definitions of the coherence lengths ξ_1 and ξ_2 :

$$\xi_1 = \frac{\hbar}{\sqrt{2m_1\alpha_1}}, \quad \xi_2 = \frac{\hbar}{\sqrt{2m_2\alpha_2}}. \quad (10)$$

The electron charge in (8) is $e < 0$; the total vector potential \mathbf{A} defines the local magnetic field \mathbf{h} :

$$\mathbf{h} = \nabla \times \mathbf{A}, \quad \mathbf{h} = (0, 0, h), \quad h = h(r). \quad (11)$$

The parameter of interband coupling, γ , may have either sign. Two-dimensional integration in the plane (r, φ) is carried out over the cross-section of the superconductor (Σ_S) in the square-bracketed terms, and over the cross-sections of the superconductor and of the opening ($\Sigma_S + \Sigma_O$) in the last (magnetic) term.

A microscopic derivation of free-energy functionals of the type (8) was given in Ref. 7 for the case of clean two-band superconductors in the limit of small interband coupling. Free-energy functionals of this type are employed in theoretical studies of different aspects of two-band superconductivity, such as, e.g., topological defects [1,3,8], current-carrying states [9], the Little-Parks effect [10], surface energy [11], etc. It should be additionally noted that, for our specific geometry and $\gamma > 0$, the functional (8) also applies to the description of a composite system consisting of two thin coaxial cylindrical films of single-band superconductors, Josephson coupled via a parallel insulating layer [12], which is exactly the experimental set-up of Ref. 2.

To obtain the actual (observable) Gibbs free energy, one has to minimize (8) with respect to Ψ , Ψ^* and \mathbf{A} under appropriate boundary conditions; however, substantial simplifications can be made already at this stage. First, we notice that, by the symmetry of the problem, the amplitudes $|\psi_1|$ and $|\psi_2|$ do not depend on φ . Moreover, they cannot depend on r , either. Indeed, by virtue of condition (2), any radial variations of $|\psi_1|$ and $|\psi_2|$ would give rise to free-energy terms that are by the factors $\xi_1^2/d^2 \gg 1$ and $\xi_2^2/d^2 \gg 1$ larger than the first and the second terms in (8), respectively, which is energetically unfavorable

[13]. As a result, in equilibrium, the magnitudes $|\psi_1|$ and $|\psi_2|$ are functions of T and H only.

Consider now the kinetic-energy terms (the first two terms in the second line of (8)). The ratio of these terms to the first and the second terms in (8), respectively, is at most of order $(\xi_1^2/R^2)(\Phi_H/\Phi_0)^2$ and $(\xi_2^2/R^2)(\Phi_H/\Phi_0)^2$, where Φ_H is the external flux, and

$$\Phi_0 = \frac{\pi\hbar c}{|e|} \quad (12)$$

is the flux quantum. Owing to condition (3), for sufficiently weak external fields, $(\xi_1^2/R^2)(\Phi_H/\Phi_0)^2$, $(\xi_2^2/R^2)(\Phi_H/\Phi_0)^2 \ll 1$. (Compare with the consideration of flux quantization in single-band superconducting cylinders [14].) In this field range, we can set $|\psi_1| = |\psi_1|_0$ and $|\psi_2| = |\psi_2|_0$, where $|\psi_1|_0$ and $|\psi_2|_0$ satisfy the equilibrium conditions for an unperturbed two-band superconductor:

$$\begin{aligned} \alpha_1 |\psi_1|_0 + \beta_1 |\psi_1|_0^3 - |\gamma| |\psi_2|_0 &= 0, \\ \alpha_2 |\psi_2|_0 + \beta_2 |\psi_2|_0^3 - |\gamma| |\psi_1|_0 &= 0. \end{aligned} \quad (13)$$

One can readily obtain a good approximate solution to (13), [15]. However, it is of no interest in the context of the soliton problem. We only note that the critical temperature, derived from (13), is $T_c = [T_1 + T_2 + \sqrt{(T_1 - T_2)^2 + \gamma^2/(a_1 a_2)}] / 2$.

In light of these simplifications, it is reasonable to consider the weak-field penetration depth [15]

$$\lambda = \frac{c}{4\sqrt{\pi}|e|} \sqrt{\frac{m_1 m_2}{m_2 |\psi_1|_0^2 + m_1 |\psi_2|_0^2}} \quad (14)$$

and to define intraband "penetration depths" [11]

$$\lambda_1 = \frac{c}{4\sqrt{\pi}|e|} \frac{\sqrt{m_1}}{|\psi_1|_0}, \quad \lambda_2 = \frac{c}{4\sqrt{\pi}|e|} \frac{\sqrt{m_2}}{|\psi_2|_0}; \quad \lambda_1^{-2} + \lambda_2^{-2} = \lambda^{-2}. \quad (15)$$

(For the above-mentioned composite, Josephson-coupled system, the quantities λ_1 and λ_2 have direct physical meaning.) We also introduce new, functionally independent phase variables ϕ and χ [9,10]:

$$\phi = \phi_1 - \phi_2, \quad (16)$$

$$\chi = c_1 \phi_1 + c_2 \phi_2; \quad c_1 \equiv (\lambda \lambda_1^{-1})^2, \quad (17)$$

$$c_2 \equiv (\lambda\lambda_2^{-1})^2, \quad c_1 + c_2 = 1.$$

Using definitions (12) and (14)–(17), we obtain the reduced Gibbs free-energy functional in the following form:

$$G[\phi, \chi, \mathbf{A}; \mathbf{H}] = F_{S0} + G_{em}[\chi, \mathbf{A}; \mathbf{H}] + F_{sol}[\phi]. \quad (18)$$

Here, the first term is the free energy of the unperturbed superconducting cylinder [10]:

$$F_{S0} = V_S \left(\alpha_1 |\psi_{10}|^2 + \alpha_2 |\psi_{20}|^2 + \frac{\beta_1}{2} |\psi_{10}|^4 + \frac{\beta_2}{2} |\psi_{20}|^4 - 2|\gamma| |\psi_{10}| |\psi_{20}| \right); \quad V_S \equiv 2\pi R L d. \quad (19)$$

The second term is the electromagnetic Gibbs free-energy functional:

$$G_{em}[\chi, \mathbf{A}; \mathbf{H}] = \frac{\Phi_0^2}{32\pi^3} \frac{L}{\lambda^2} \int_{\Sigma_S} d^2\mathbf{r} \left(\nabla\chi - \frac{2e}{\hbar c} \mathbf{A} \right)^2 + \frac{L}{8\pi} \int_{\Sigma_S + \Sigma_O} d^2\mathbf{r} (\mathbf{h} - \mathbf{H})^2, \quad (20)$$

with the first term on the right-hand side of (20) being the kinetic-energy functional of the supercurrent. Finally, the last term in (18) is

$$F_{sol}[\phi] = \frac{\Phi_0^2}{32\pi^3} \frac{L}{\lambda^2} c_1 c_2 \int_{\Sigma_S} d^2\mathbf{r} \left[(\nabla\phi)^2 + \frac{2}{l^2} (1 - \text{sgn } \gamma \cos \phi) \right]; \quad (21)$$

$$l^2 \equiv \frac{\Phi_0^2}{32\pi^3} \frac{1}{\lambda^2} \frac{c_1 c_2}{|\gamma| |\psi_{10}| |\psi_{20}|},$$

where $\text{sgn } x$ is the sign function. The term (21) should be interpreted as the soliton self-energy functional. Indeed, when $n_1 = n_2$ in (7), we have [9,10] either $\phi = 0 \pmod{2\pi}$ (for $\gamma > 0$) or $\phi = \pi \pmod{2\pi}$ (for $\gamma < 0$), and this term vanishes identically.

Our task now is to minimize (18) with respect to ϕ , χ and \mathbf{A} . As the phase variable ϕ is not coupled to the vector potential \mathbf{A} , this procedure can be performed in two separate steps.

3. Electromagnetic Gibbs free energy

The minimization of the electromagnetic functional (20) reduces to evaluation of the stationarity condition $\delta G_{em} = 0$, or, in terms of functional derivatives,

$$\frac{\delta G_{em}}{\delta \mathbf{A}} = 0, \quad \frac{\delta G_{em}}{\delta \chi} = 0. \quad (22)$$

Indeed, in view of quadratic nature of (20), solutions to (22) are automatically minimizers of this functional (i.e., the second variation $\delta^2 G_{em} > 0$ at these solutions).

Variation with respect to \mathbf{A} yields Ampère's law

$$\nabla \times \nabla \times \mathbf{A} = 0, \quad r \in (0, r_1); \quad (23)$$

$$\nabla \times \nabla \times \mathbf{A} = \frac{4\pi}{c} \mathbf{j}, \quad r \in (r_1, r_2), \quad (24)$$

with

$$\mathbf{j} = -\frac{c}{4\pi\lambda^2} \left(\frac{\Phi_0}{2\pi} \nabla\chi + \mathbf{A} \right) \quad (25)$$

being the supercurrent density ($\mathbf{j} = (0, j, 0)$ by symmetry), and the boundary condition

$$\mathbf{h}|_{r=r_2} \equiv \nabla \times \mathbf{A}|_{r=r_2} = \mathbf{H}. \quad (26)$$

(This boundary condition should, of course, be complemented by the conditions of continuity of \mathbf{A} and \mathbf{h} at $r = r_2$ and the condition of regularity of \mathbf{A} at the origin.) Variation with respect to χ , under the condition of single-valuedness of variations $\delta\chi$, just yields the current-conservation law

$$\nabla \mathbf{j} = 0 \quad (27)$$

and the single-valuedness condition

$$j|_{\varphi=0} = j|_{\varphi=2\pi}. \quad (28)$$

(This boundary condition should be complemented by a condition on χ resulting from (7).)

The problem of finding \mathbf{A} and χ is still sub-definite, because we have not so far fixed the gauge. As the z component of the vector potential drops out of the definition of \mathbf{h} (see (11)), it is equal to an arbitrary constant, and we set $A_z \equiv 0$. The r component of the vector potential can be eliminated by the gauge transformation

$$\mathbf{A} \rightarrow \mathbf{A} - \nabla \int_0^r A_r(r', \varphi) dr', \quad \chi \rightarrow \chi + \frac{2\pi}{\Phi_0} \int_0^r A_r(r', \varphi) dr'.$$

In this particular gauge,

$$\mathbf{A} = (0, A, 0), \quad A = A(r); \quad (29)$$

$$h = \frac{1}{r} \frac{d}{dr} (rA), \quad (30)$$

and χ does not depend on r ($j_r \equiv 0$). Using (7), (17), (27) and (28), we arrive at a well-posed boundary-value problem,

$$\frac{d^2\chi}{d\varphi^2} = 0, \quad \varphi \in (0, 2\pi);$$

$$\chi(2\pi) = \chi(0) + 2\pi(n_1 c_1 + n_2 c_2), \quad \frac{d\chi}{d\varphi}(2\pi) = \frac{d\chi}{d\varphi}(0),$$

whose solution is

$$\chi(\varphi) = (n_1 c_1 + n_2 c_2) \varphi + \varphi_0, \quad (31)$$

with φ_0 being an arbitrary constant.

The boundary-value problem for the vector potential now takes the form

$$\begin{aligned} \frac{d}{dr} \left[\frac{1}{r} \frac{d}{dr} (rA) \right] &= 0, \quad r \in (0, r_1); \\ \frac{d}{dr} \left[\frac{1}{r} \frac{d}{dr} (rA) \right] &= \frac{1}{\lambda^2} \left[A + \frac{\Phi_0}{2\pi} q(n_1, n_2) \right], \quad r \in (r_1, r_2); \\ q(n_1, n_2) &\equiv n_1 c_1 + n_2 c_2; \\ |A|_{r=0} < \infty, \quad A|_{r=r_1-0} &= A|_{r=r_1+0}, \quad \frac{1}{r} \frac{d}{dr} (rA) \Big|_{r=r_1-0} = \\ &= \frac{1}{r} \frac{d}{dr} (rA) \Big|_{r=r_1+0}, \quad \frac{1}{r} \frac{d}{dr} (rA) \Big|_{r=r_2} = H. \end{aligned} \quad (32)$$

This boundary-value problem admits an exact solution: it is presented in Appendix 1. However, to obtain a second-order expansion of the electromagnetic Gibbs free energy in terms of the small parameter ε (see Introduction), we need only first-order expansions of A and h . They are as follows:

$$A(r) = \begin{cases} \frac{r}{2} H - \frac{r}{2} \left[\frac{\Phi_0}{\pi r_1^2} q(n_1, n_2) + H \right] \varepsilon, & r \in [0, r_1]; \\ \frac{r}{2} H - \frac{r_1}{2} \left[\frac{\Phi_0}{\pi r_1^2} q(n_1, n_2) + H \right] \varepsilon, & r \in (r_1, r_2]; \end{cases} \quad (33)$$

$$h(r) = \begin{cases} H - \left[\frac{\Phi_0}{\pi r_1^2} q(n_1, n_2) + H \right] \varepsilon, & r \in [0, r_1]; \\ H - \frac{r_2 - r}{r_2 - r_1} \left[\frac{\Phi_0}{\pi r_1^2} q(n_1, n_2) + H \right] \varepsilon, & r \in (r_1, r_2]. \end{cases} \quad (34)$$

(The fact that expressions (33) and (34) on the interval (r_1, r_2) are not related to each other by equation (30) should not cause any confusion: to ensure the fulfillment of (30), we would have to continue the expansion of (61) up to small terms of order d/R and $\varepsilon(d/R)$.)

Bearing in mind that in integral physical quantities any difference between r_1 , r_2 and R should be neglected [see (65)], by use of equations (34) and (24) we obtain expressions for the total flux $\Phi = \int_{\Sigma_0} h d^2 \mathbf{r}$ and the total super-

$$\begin{aligned} \text{current } J &= L \int_{r_1}^{r_2} j dr; \\ \Phi &= \Phi_H + \Phi_i, \quad \Phi_H = \pi R^2 H, \end{aligned} \quad (35)$$

$$\Phi_i = -[\Phi_0 q(n_1, n_2) + \Phi_H] \varepsilon;$$

$$J = \frac{c}{\mathcal{L}_m} \Phi_i, \quad \mathcal{L}_m = \frac{4\pi^2 R^2}{L}. \quad (36)$$

Here, Φ_H and Φ_i are the external and self-induced flux, respectively; \mathcal{L}_m is the magnetic inductance of the cylinder (or self-inductance) [16].

On substitution of relations (31), (33) and (34) into (20), we get the electromagnetic Gibbs free energy of the state parameterized by topological numbers n_1 and n_2 :

$$\begin{aligned} G_{em}(n_1, n_2; H) &= \frac{[\Phi_0 q(n_1, n_2) + \Phi_H]^2}{2\mathcal{L}_m} \varepsilon(1 - 2\varepsilon) + \\ &+ \frac{[\Phi_0 q(n_1, n_2) + \Phi_H]^2}{2\mathcal{L}_m} \varepsilon^2 = \\ &= \frac{\Phi_0^2 \varepsilon}{2\mathcal{L}_m} [q(n_1, n_2) + f_H]^2 (1 - \varepsilon), \quad f_H \equiv \frac{\Phi_H}{\Phi_0}. \end{aligned} \quad (37)$$

(Note that the first term in the first line of this equation is the kinetic energy of the supercurrent, whereas the second term in the same line is the magnetic Gibbs free energy.)

To facilitate an analysis of soliton states, we should transform (37) to a more convenient form. First, instead of parameterization by n_1 and n_2 , we introduce parameterization by n_1 and the soliton number $n = n_1 - n_2$. From now on, we assume (without any loss of generality) that $0 < c_2 \leq c_1 < 1$. Relation (37) is rewritten as follows:

$$G_{em}(n_1, n; f_H) = \frac{\Phi_0^2 \varepsilon}{2\mathcal{L}_m} (f_H + n_1 - n c_2)^2 (1 - \varepsilon). \quad (38)$$

From a thermodynamic point of view, of interest is the minimum of (38) for given $|n| = 0, 1, 2, \dots$. Therefore, relation (38) should be minimized with respect to n_1 and $\text{sgn } n$. With this in mind, we introduce two discontinuous functions, a step function $m(x)$ and a periodic function $\theta(x)$, via the definitions

$$m(x) = \begin{cases} [x], & 0 \leq \{x\} \leq \frac{1}{2}; \\ [x] + 1, & \frac{1}{2} < \{x\} < 1, \end{cases} \quad (39)$$

and

$$\theta(x) = \begin{cases} \{x\}, & 0 \leq \{x\} \leq \frac{1}{2}; \\ -1 + \{x\}, & \frac{1}{2} < \{x\} < 1, \end{cases} \quad (40)$$

where $[x]$ and $\{x\}$ are the integer and fractional parts of x , respectively. Given that f_H and $n c_2$ can now be represented as $f_H = m(f_H) + \theta(f_H)$ and $n c_2 = \text{sgn } n [m(|n| c_2) + \theta(|n| c_2)]$, respectively, the result of the minimization is

$$G_{em}(|n|; f_H) = \begin{cases} \min_{n_1, \text{sgn } n} G_{em}(n_1, n; f_H), \\ G_{em}(-m(f_H) + m(|n|c_2) \text{sgn } \theta(f_H) \text{sgn } \theta(|n|c_2), |n| \text{sgn } \theta(f_H) \text{sgn } \theta(|n|c_2); f_H), \\ \frac{\Phi_0^2 \varepsilon}{2\mathcal{L}_m} \left[|\theta(f_H)| - |\theta(|n|c_2)| \right]^2 (1 - \varepsilon). \end{cases} \quad (41)$$

4. Soliton states

4.1. Soliton self-energy

The variation of (21) with respect to ϕ , under the condition of single-valuedness of variations $\delta\phi$, yields a static two-dimensional sine-Gordon equation in polar coordinates,

$$\frac{1}{r^2} \frac{\partial^2 \phi}{\partial \varphi^2} + \frac{1}{r} \frac{\partial}{\partial r} \left(r \frac{\partial \phi}{\partial r} \right) = \frac{\text{sgn } \gamma}{l^2} \sin \phi, \quad (42)$$

$$r \in (r_1, r_2), \quad \varphi \in (0, 2\pi),$$

and the boundary conditions

$$\left. \frac{1}{r} \frac{\partial \phi}{\partial \varphi} \right|_{\varphi=0} = \left. \frac{1}{r} \frac{\partial \phi}{\partial \varphi} \right|_{\varphi=2\pi}; \quad \left. \frac{\partial \phi}{\partial r} \right|_{r=r_1} = \left. \frac{\partial \phi}{\partial r} \right|_{r=r_2} = 0. \quad (43)$$

(These boundary conditions should, of course, be complemented by a condition on ϕ resulting from (7).)

However, equation (42), in its exact form, by far exceeds the accuracy of our calculations in the previous section (see expressions (33), (34) and relations (65)). Discarding in (42) terms of order d/R and d^2/R^2 , we arrive at a two-dimensional sine-Gordon equation in "Cartesian coordinates":

$$\frac{\partial^2 \phi}{\partial \rho^2} + \frac{\partial^2 \phi}{\partial \rho^2} = \frac{R^2 \text{sgn } \gamma}{l^2} \sin \phi, \quad \rho \equiv \frac{r}{R}. \quad (44)$$

Solutions to (44), minimizing the functional (21), should not depend on ρ for symmetry reasons (which, of course, is compatible with boundary conditions (43)).

Thus, the phase $\phi = \phi(\varphi)$ satisfies the following boundary-value problem:

$$\frac{d^2 \phi}{d\varphi^2} = \frac{R^2 \text{sgn } \gamma}{l^2} \sin \phi, \quad \varphi \in (0, 2\pi);$$

$$\phi(2\pi) = \phi(0) + 2\pi n \quad (n = \pm 1, \pm 2, \dots),$$

$$\frac{d\phi}{d\varphi}(2\pi) = \frac{d\phi}{d\varphi}(0). \quad (45)$$

The solution of (45) is straightforward [17,18]:

$$\phi_n(\varphi) = \frac{(1 + \text{sgn } \gamma)}{2} + 2\text{am} \left(\frac{nK(k_n)}{\pi} (\varphi - \varphi_{n0}), k_n \right), \quad (46)$$

where an u is the elliptic amplitude [19], $K(k)$ is the complete elliptic integral of the first kind [19], φ_{n0} are arbitrary constants, and k_n ($n = \pm 1, \pm 2, \dots$) satisfy the equations

$$|n|k_n K(k_n) = \frac{\pi R}{l}, \quad n = \pm 1, \pm 2, \dots \quad (47)$$

Particular examples of solutions (46) that possess asymptotics in terms of elementary functions are relegated to Appendix 3. Nonetheless, the very special class of exact elementary solutions is worth being presented here: namely, the non-soliton nontrivial topological solutions corresponding to the physical case of the absence of interband coupling ($|\gamma| = 0$). These solutions can be obtained from (46) by the limit procedure

$$k_n \rightarrow 0, \quad n = \pm 1, \pm 2, \dots, \quad (48)$$

and they have the general form

$$\phi_n(\varphi) = n\varphi + \varphi_0. \quad (49)$$

They are necessarily minimizers of (21) [i.e., at these solutions $\delta^2 F_{\text{sol}} > 0$, because the functional (21) is quadratic in the case $|\gamma| = 0$], and their self-energy is

$$F_{\text{sol}}^{(0)}(n) = \lim_{k_n \rightarrow 0} F_{\text{sol}}(n) = \frac{\Phi_0^2 \varepsilon}{2\mathcal{L}_m} |n|^2 c_1 c_2. \quad (50)$$

If $|\gamma| \neq 0$, the functional (21) is non-quadratic, and we should analyze the second variation of (21) in more detail. To this end, [18,20] we turn to the Sturm–Liouville problem

$$-\frac{d^2 \psi}{d\varphi^2} + \cos \phi_n \psi = \mu \psi, \quad \varphi \in (0, 2\pi); \quad (51)$$

$$\psi(0) = \psi(2\pi), \quad \frac{d\psi}{d\varphi}(0) = \frac{d\psi}{d\varphi}(2\pi),$$

where ϕ_n is a given solution from the set (46). As shown in Refs. 18,20,

$$\delta^2 F_{\text{sol}} \Big|_{\phi=\phi_n} \geq \mu_0 \int_0^{2\pi} |\delta\phi_n|^2 d\varphi,$$

where μ_0 is lowest eigenvalue of the problem (51). In our case, both μ_0 and the corresponding eigenfunction ψ_0 can be readily found:

$$\mu_0 = 0, \quad \psi_0 = \text{const dn} \left(\frac{nK(k_n)}{\pi} (\varphi - \varphi_{n0}), k_n \right),$$

where $dn u = damu / du$ [19]. This means that $\delta^2 F_{sol}|_{\phi=\phi_n} \geq 0$, and soliton states turn out to be indifferently stable states. Indeed, the zero value of μ_0 should be attributed to the existence of a zero-frequency "rotational mode" (by analogy with the well-known [21] translational mode in field theories) that restores rotational symmetry broken by the formation of solitons. To prove this, consider a small variation of ϕ_n induced by a small variation of the constant of integration ϕ_{n0} :

$$\begin{aligned} \phi_n(\varphi) &\rightarrow \phi_n\left(\varphi + \frac{\pi}{nK} \alpha\right) \approx \\ &\approx \phi_n(\varphi) + \alpha dn\left(\frac{nK(k_n)}{\pi}(\varphi - \phi_{n0}), k_n\right), \quad |\alpha| \ll 1. \end{aligned}$$

From the above, we see that $\delta\phi_n \propto \psi_0$.

Now that local stability of soliton solutions is established, we proceed with a discussion of soliton self-energy. It is obtained by the substitution of solutions (46) into (21) and has the form

$$F_{sol}(n) = \frac{\Phi_0^2 \varepsilon}{\mathcal{L}_m} \frac{2|n|^2}{\pi^2} c_1 c_2 K(k_n) \left[2E(k_n) - (1 - k_n^2) K(k_n) \right], \tag{52}$$

where $E(k)$ is the complete elliptic integral of the second kind [19].

First, we note that the constants of integration ϕ_{n0} that figure in (46) drop out of the right-hand side of (52), as they should. The self-energy does not depend on the sign of γ and of n , either. By considering (formally) $|n|$ as a continuous variable, we get

$$\frac{\partial F_{sol}(n)}{\partial |n|} = \frac{\Phi_0^2 \varepsilon}{\mathcal{L}_m} \frac{4|n|R}{\pi l} c_1 c_2 E(k_n) > 0,$$

which means that $F_{sol}(n)$ increases monotonically with an increase in $|n|$, as could be expected. However, in contrast to the case $|\gamma| = 0$ (see (50)), the growth of $F_{sol}(n)$ is slower than $|n|^2$, because

$$\frac{\partial}{\partial |n|} \left[\frac{F_{sol}(n)}{|n|^2} \right] = - \frac{\Phi_0^2 \varepsilon}{\mathcal{L}_m} \frac{4R}{\pi |n|^2 l} c_1 c_2 \frac{E(k_n) - (1 - k_n^2) K(k_n)}{k_n} < 0.$$

Given that

$$\frac{\partial F_{sol}(n)}{\partial k_n} = \frac{\Phi_0^2 \varepsilon}{\mathcal{L}_m} \frac{4|n|^2}{\pi^2} c_1 c_2 \frac{E(k_n) \left[E(k_n) - (1 - k_n^2) K(k_n) \right]}{k_n (1 - k_n^2)} > 0, \quad k_n \in (0, 1),$$

the self-energy increases monotonically with an increase in k_n on the whole interval $(0, 1)$. The minimal value of (52) is achieved at $k_n = 0$ and is given by (50). In view of the relation

$$\frac{\partial k_n}{\partial \left(\frac{l}{R}\right)} = - \frac{\pi R^2}{|n|^2 l^2} \frac{1 - k_n^2}{E(k_n)} < 0,$$

the self-energy decreases monotonically with an increase in $(l/R) \in (0, \infty)$ (for a given $|n|$). (In other words, F_{sol} is an increasing function of the interband coupling parameter $|\gamma|$: see the definition of l in (21).)

To analyze thermodynamic stability of soliton solutions, we should compare expression (53) for $|n| \geq 1$ with the Gibbs free energy of the states with $|n| = 0$:

$$G(0; f_H) = F_0 + \frac{\Phi_0^2 \varepsilon}{2\mathcal{L}_m} |\theta(f_H)|^2 (1 - \varepsilon). \tag{54}$$

4.2. Thermodynamic metastability

According to (18), (41) and (52) the minimal Gibbs free energy of soliton states with a given $|n|$ in the field H can be represented as follows:

$$\begin{aligned} G(|n|; f_H) &= F_0 + \frac{\Phi_0^2 \varepsilon}{2\mathcal{L}_m} \left[\left[|\theta(f_H)| - |\theta(|n|c_2)| \right]^2 (1 - \varepsilon) + \right. \\ &\left. + \frac{4|n|^2}{\pi^2} c_1 c_2 K(k_n) \left[2E(k_n) - (1 - k_n^2) K(k_n) \right] \right]. \tag{53} \end{aligned}$$

With this in mind, we first note that, for $|n| \geq 1$, the energy $G(|n|; f_H)$ increases monotonically with an increase in $|n|$: see Appendix 2 for a proof. (Contrary to what may seem, this fact is by no means obvious, because the electromagnetic term in (53) may decrease with an increase in $|n|$.) Furthermore, since expression (50) pro-

vides the greatest lower bound for soliton self-energies, we can restrict ourselves to the case $|n|=1$ and $k_n=0$. Bearing in mind that $c_2 \in (0, 1/2]$ by assumption (see the end of Section 3), we arrive at the following important inequalities:

$$\begin{aligned} \Delta G(1; f_H) &\equiv G(1; f_H) - G(0; f_H) \geq \\ &\geq \Delta G^{(0)}(1; f_H) \equiv \lim_{k_n \rightarrow 0} G(1; f_H) - G(0; f_H) = \\ &= \frac{\Phi_0^2 \varepsilon}{2\mathcal{L}_m} c_2 [1 - c_2 \varepsilon - 2|\theta(f_H)|(1 - \varepsilon)] > 0. \end{aligned} \quad (55)$$

The above inequalities clearly demonstrate thermodynamic metastability of soliton states and bring to light certain subtle physical points. In particular,

$$\begin{aligned} \max_{f_H} \Delta G(1; f_H) &= \Delta G(1; f_H) \Big|_{f_H=p} \geq \\ &\geq \frac{\Phi_0^2 \varepsilon}{2\mathcal{L}_m} c_2 (1 - c_2 \varepsilon), \quad p = 0, 1, 2, \dots \end{aligned} \quad (56)$$

In contrast,

$$\begin{aligned} \min_{f_H} \Delta G(1; f_H) &= \Delta G(1; f_H) \Big|_{f_H=p+\frac{1}{2}} \geq \\ &\geq \frac{\Phi_0^2 \varepsilon^2}{2\mathcal{L}_m} c_1 c_2, \quad p = 0, 1, 2, \dots, \end{aligned} \quad (57)$$

which shows that $\min_{f_H} \Delta G(1; f_H)$ can be much smaller than the magnetic Gibbs free energy of the zero-soliton states [see (37)], provided that $0 < c_2 \ll c_1 < 1$ (i.e., when $\lambda_1 \ll \lambda_2 < \infty$, see (17)) and $(l/R) \gg 1$ (weak interband coupling).

In Fig. 2, we plot the Gibbs free energy of several different topological states (n_1, n) ($|n|=0, 1, 2$). Thermodynamically stable zero-soliton states are denoted by thick solid lines. Minima of the Gibbs free energy of soliton states represent the soliton self-energy and occur when the self-induced flux Φ_i compensates for the external flux Φ_H , i.e., when

$$f_H + n_1 - n c_2 = 0,$$

(see relations (35), (38) and (41)). In the very special case, when $c_2 = c_1 = 1/2$ and $n = 2n_1$, no flux is induced ($\Phi_i = 0$), and minima of the soliton Gibbs free energy occur at $H = 0$.

5. Summary and conclusions

Summarizing, we have presented (in the framework of the Ginzburg-Landau approach) a self-consistent theory of specific soliton states that constitute a distinctive feature of two-band superconductivity in mesoscopic multiply-connected samples. Although our mathematical consideration concerns the concrete geometry of Fig. 1, the final results can be expressed in terms of the magnetic and kinetic inductance (see Ref. 16) and, therefore, should apply to a much wider class of structures. This allows us to make several generalizing remarks.

As the predicted fractional magnetic vortices in bulk two-band superconduct [3], the soliton states considered here prove to be thermodynamically metastable. However, the minimal energy gap between the lowest-lying single-soliton states and thermodynamically stable zero-soliton states can be much smaller than the magnetic Gibbs free energy of the latter states, provided that the intraband "penetration depths" (15) differ substantially and the interband coupling is weak. (In order to establish this important physical fact, we had to evaluate self-consistently the vector potential. The results of this evaluation may be of interest in themselves.)

Our consideration encompasses in a natural way the case of superconducting Josephson-coupled bilayer structures studied experimentally in Ref. 2. Our conclusion that the self-energy of soliton states increases monotonically with an increase in the strength of interband coupling qualitatively agrees with the observations reported therein.

Furthermore, as a particular limit, our consideration contains the case of zero interband coupling. In view of the recently discussed possibility of independent superconductivity of electrons and protons in a liquid metallic state of hydrogen [22], some of our results may find application in this situation as well.

Finally, the exact soliton solutions derived in this paper should be compared with the exact soliton solutions representing equilibrium Josephson vortices in a superconducting tunnel junction [18,20]. In particular, Josephson vortices are pinned in their equilibrium positions owing to interaction with the edges of the junction. In contrast, in rotationally symmetric doubly-connected two-band superconductors, soliton positions are not fixed, which gives rise to a specific zero-frequency rotational mode. However, any defects that break rotational symmetry must cause soliton pinning. The effect of this pinning is outside the scope of the present paper and requires a separate discussion. In conclusion, we hope that our paper will stimulate further experimental and theoretical studies of the intriguing phenomenon of soliton states in two-band superconductors.

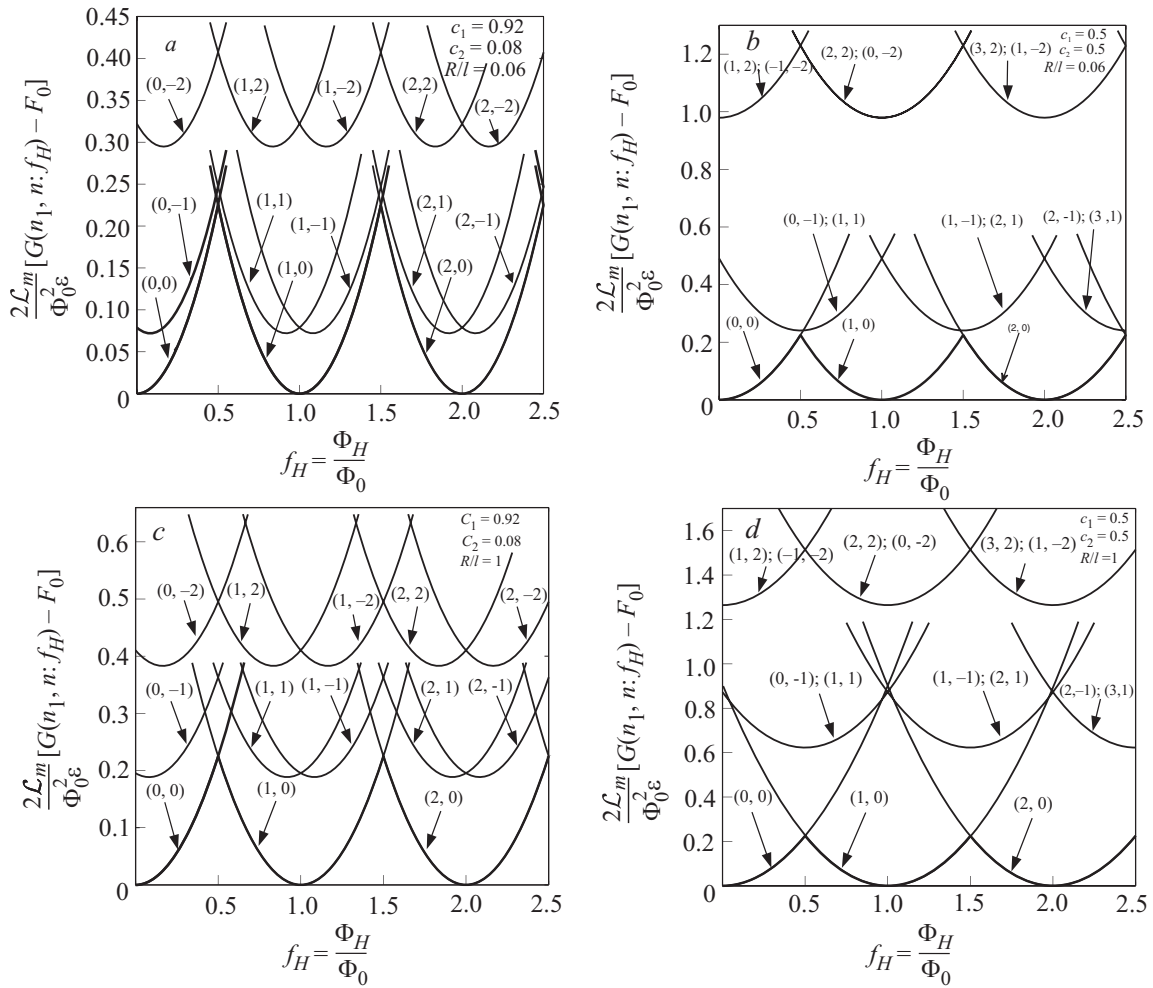


Fig. 2. Gibbs free energy of several different topological states (n_1, n) ($|n| = 0, 1, 2$) for typical values of the parameters c_1, c_2 , and R/l . Note double degeneracy of soliton states in the case $c_2 = c_2 = 1/2$ and see the text for further explanations.

Appendix 1: Exact solution of the boundary-value problem for the vector potential

The exact solution to (32) has the following form:

$$A(r) = \begin{cases} \frac{rh_0}{2}, & r \in [0, r_1]; \\ -\frac{\Phi_0}{2\pi r} q(n_1, n_2) + C_1 I_1\left(\frac{r}{\lambda}\right) + C_2 K_1\left(\frac{r}{\lambda}\right), & r \in (r_1, r_2]; \end{cases} \tag{A1.1}$$

$$h(r) = \begin{cases} h_0, & r \in [0, r_1]; \\ \frac{C_1}{\lambda} I_0\left(\frac{r}{\lambda}\right) - \frac{C_2}{\lambda} K_0\left(\frac{r}{\lambda}\right), & r \in (r_1, r_2]; \end{cases} \tag{A1.2}$$

$$h_0 = \frac{2\lambda H f_2\left(\frac{r_1}{\lambda}, \frac{r_1}{\lambda}\right) \Phi_0 q(n_1, n_2) f_1\left(\frac{r_2}{\lambda}, \frac{r_1}{\lambda}\right)}{r_1 f_1\left(\frac{r_2}{\lambda}, \frac{r_1}{\lambda}\right) + 2\lambda f_2\left(\frac{r_2}{\lambda}, \frac{r_1}{\lambda}\right) - \pi r_1 \left[r_1 f_1\left(\frac{r_2}{\lambda}, \frac{r_1}{\lambda}\right) + 2\lambda f_2\left(\frac{r_2}{\lambda}, \frac{r_1}{\lambda}\right) \right]}; \tag{A1.3}$$

$$C_1 \equiv \frac{\lambda H \left[r_1 K_0 \left(\frac{r_1}{\lambda} \right) + 2\lambda K_1 \left(\frac{r_1}{\lambda} \right) \right]}{r_1 f_1 \left(\frac{r_2}{\lambda}, \frac{r_1}{\lambda} \right) + 2\lambda f_2 \left(\frac{r_2}{\lambda}, \frac{r_1}{\lambda} \right)} + \frac{\lambda \Phi_0 q(n_1, n_2) K_0 \left(\frac{r_2}{\lambda} \right)}{\pi r_1 \left[r_1 f_1 \left(\frac{r_2}{\lambda}, \frac{r_1}{\lambda} \right) + 2\lambda f_2 \left(\frac{r_2}{\lambda}, \frac{r_1}{\lambda} \right) \right]},$$

$$C_2 \equiv \frac{\lambda H \left[r_1 I_0 \left(\frac{r_1}{\lambda} \right) - 2\lambda I_1 \left(\frac{r_1}{\lambda} \right) \right]}{r_1 f_1 \left(\frac{r_2}{\lambda}, \frac{r_1}{\lambda} \right) + 2\lambda f_2 \left(\frac{r_2}{\lambda}, \frac{r_1}{\lambda} \right)} + \frac{\lambda \Phi_0 q(n_1, n_2) I_0 \left(\frac{r_2}{\lambda} \right)}{\pi r_1 \left[r_1 f_1 \left(\frac{r_2}{\lambda}, \frac{r_1}{\lambda} \right) + 2\lambda f_2 \left(\frac{r_2}{\lambda}, \frac{r_1}{\lambda} \right) \right]};$$

$$f_1(x, y) \equiv I_0(x)K_0(y) - I_0(y)K_0(x), \quad f_2(x, y) \equiv I_0(x)K_1(y) + I_1(y)K_0(x).$$

Here, $I_\nu(x)$ and $K_\nu(x)$ are modified Bessel functions of order $\nu = 0, 1$ [19]; h_0 is the constant magnetic field in the opening. Expressions (A1.1)–(A1.3) are greatly simplified under condition (4):

$$A(r) = \begin{cases} \frac{rh_0}{2}, & r \in [0, r_1]; \\ \frac{\Phi_0 q(n_1, n_2)}{2\pi r} \frac{\sinh \frac{d}{\lambda} + \frac{2\lambda}{r_1} \left(\cosh \frac{d}{\lambda} - \sqrt{\frac{r}{r_1}} \cosh \frac{r_2 - r}{\lambda} \right)}{\sinh \frac{d}{\lambda} + \frac{2\lambda}{r_1} \cosh \frac{d}{\lambda}} + \lambda H \sqrt{\frac{r_2}{r}} \frac{\cosh \frac{r - r_1}{\lambda} + \frac{2\lambda}{r_1} \sinh \frac{r - r_1}{\lambda}}{\sinh \frac{d}{\lambda} + \frac{2\lambda}{r_1} \cosh \frac{d}{\lambda}}, & r \in (r_1, r_2]; \end{cases} \quad (\text{A1.4})$$

$$h(r) = \begin{cases} h_0, & r \in [0, r_1]; \\ \frac{\Phi_0 q(n_1, n_2)}{\pi r_1 \sqrt{r r_1}} \frac{\sinh \frac{r_2 - r}{\lambda}}{\sinh \frac{d}{\lambda} + \frac{2\lambda}{r_1} \cosh \frac{d}{\lambda}} + H \sqrt{\frac{r_2}{r}} \frac{\sinh \frac{r - r_1}{\lambda} + \frac{2\lambda}{r_1} \cosh \frac{r - r_1}{\lambda}}{\sinh \frac{d}{\lambda} + \frac{2\lambda}{r_1} \cosh \frac{d}{\lambda}}, & r \in (r_1, r_2]; \end{cases} \quad (\text{A1.5})$$

$$h_0 = \frac{-\frac{\Phi_0 q(n_1, n_2)}{\pi r_1^2} \sinh \frac{d}{\lambda} + \frac{2\lambda}{r_1} \sqrt{\frac{r_2}{r_1}} H}{\sinh \frac{d}{\lambda} + \frac{2\lambda}{r_1} \cosh \frac{d}{\lambda}}. \quad (\text{A1.6})$$

Expressions (A1.4)–(A1.6) should be compared with analogous expressions for a single-band-superconducting cylinder [14]. As can be easily seen, the cylinder exhibits a considerable Meissner effect under the conditions

$$\frac{d}{\lambda} \ll 1, \quad \frac{dR}{2\lambda^2} \gg 1. \quad (\text{A1.7})$$

In contrast, in the opposite case, when condition (5) is fulfilled, the Meissner effect is small, and expressions (A1.4)–(A1.6) can be readily expanded up to first-order terms in ε . Taking into account a hierarchy of the small parameters of the problem,

$$\frac{d}{r_1} \approx \frac{d}{r_2} \approx \frac{d}{R} \equiv 2\varepsilon \frac{\lambda^2}{R^2}, \quad \frac{d}{\lambda} \equiv 2\varepsilon \frac{\lambda}{R};$$

$$\frac{d}{R} \ll \frac{d}{\lambda} \ll \varepsilon, \quad \frac{\lambda}{R} \ll 1, \quad (\text{A1.8})$$

we arrive at the first-order expressions (33) and (34).

Appendix 2: A proof of the inequality

$$G(|n|; f_H) \Big|_{|n|>1} > G(1; f_H)$$

Consider the expression

$$\begin{aligned} \frac{2\mathcal{L}_m}{\Phi_0^2 \varepsilon} \Delta G(|n|; f_H) &\equiv \frac{2\mathcal{L}_m}{\Phi_0^2 \varepsilon} [G(|n|; f_H) - G(0; f_H)] = \\ &= -|\theta(|n|c_2)| [2|\theta(f_H)| - |\theta(|n|c_2)|] (1 - \varepsilon) + \\ &+ \frac{4|n|^2}{\pi^2} c_1 c_2 K(k_n) [2E(k_n) - (1 - k_n^2)K(k_n)] \end{aligned} \quad (\text{A2.1})$$

that follows directly from (53). Our task is to prove that the right-hand side of (A2.1) for $|n| > 1$ is larger than for $|n| = 1$. Given that $c_2 \in (0, 1/2]$ by assumption (see the

end of Sec. 3), it is sufficient to provide a proof for $1 < |n| \leq [1/2c_2] + 1$, where $[1/2c_2]$ is the integer part of $1/2c_2$. Indeed, the first term on the right-hand side of (A2.1) satisfies the inequality

$$\left| \theta(|n|c_2) \left[2|\theta(f_H)| - \theta(|n|c_2) \right] (1-\varepsilon) \right| \leq \frac{1}{4}(1-\varepsilon),$$

whereas

$$\frac{4K(k_n)}{\pi^2} \left[2E(k_n) - (1-k_n^2)K(k_n) \right] \geq 1.$$

Therefore, for $|n| > \left[\frac{1}{2c_2} \right] + 1$, when $|n|c_2 > \frac{1}{2}$, any possible decrease in the first term on the right-hand side of (66) due to an increase in $|n|$ cannot compensate for an incurred increase in the second term.

For $1 < |n| < [1/2c_2] + 1$, there holds the relation $|n|c_2 \leq 1/2$, and (A2.1) becomes

$$\frac{2\mathcal{L}_m}{\Phi_0^2\varepsilon} \Delta G(|n|; f_H) \Big|_{|n|>1} = \begin{cases} |n|c_2 \left[|n|(1-c_2\varepsilon) - 2|\theta(f_H)|(1-\varepsilon) \right] + |n|^2 c_1 c_2 \left[\frac{4K(k_n)}{\pi^2} \left[2E(k_n) - (1-k_n^2)K(k_n) \right] - 1 \right] \\ |n| \frac{2\mathcal{L}_m}{\Phi_0^2\varepsilon} \Delta G(1; f_H) + c_2 |n| (|n|-1) \left[(1-c_2\varepsilon) + \frac{4c_1 K(k_n)}{\pi^2} \left[2E(k_n) - (1-k_n^2)K(k_n) \right] - c_1 \right] \\ > \frac{2\mathcal{L}_m}{\Phi_0^2\varepsilon} \Delta G(1; f_H), \end{cases}$$

which was to be proved.

Appendix 3: Particular examples of soliton solutions

In Fig. 3, we present several different soliton solutions

obtained numerically. (For greater clarity, we plot the derivatives $d\phi_n/d\varphi$.) However, in two limiting cases soliton solutions possess asymptotics in terms of elementary func-

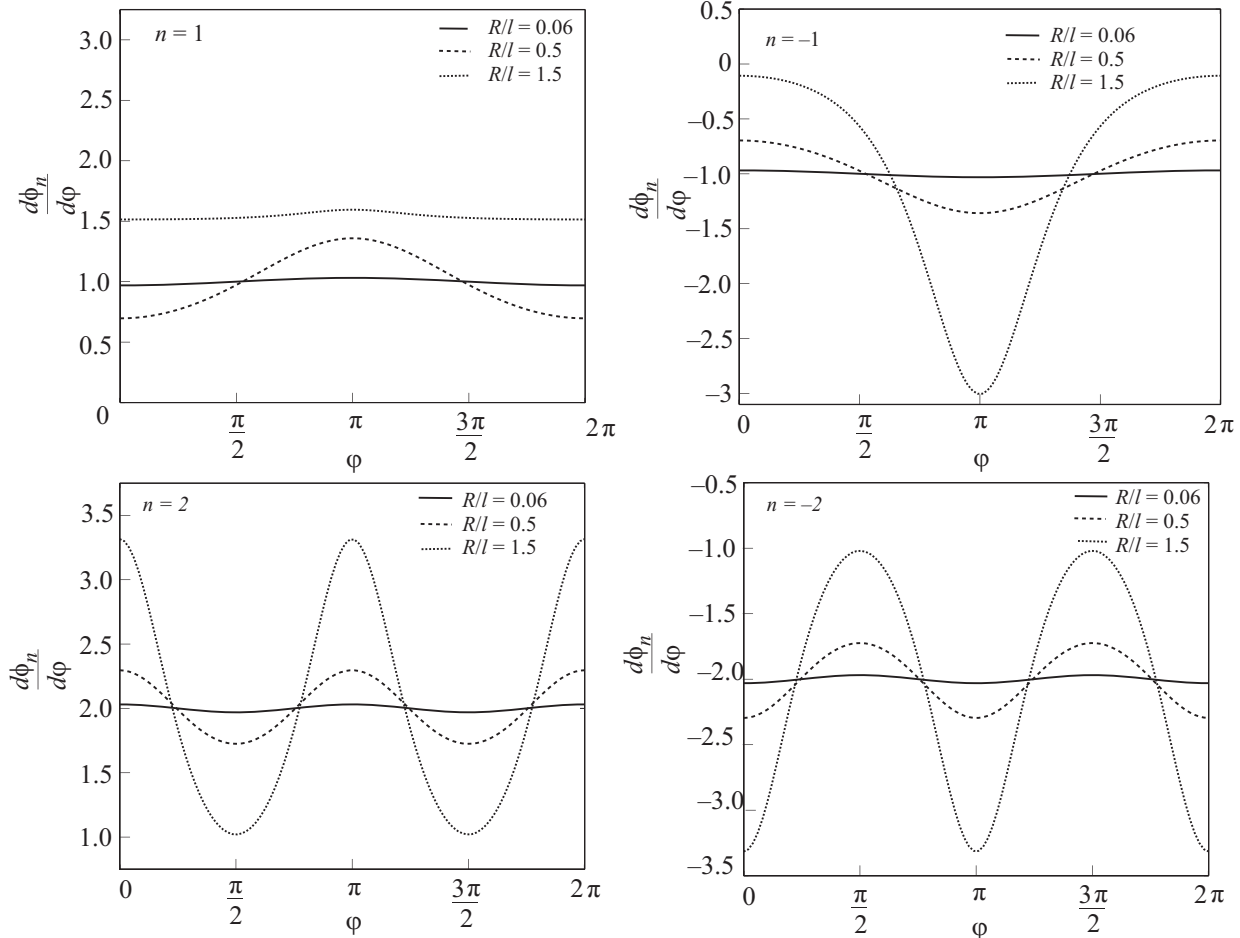


Fig. 3. Particular examples of soliton solutions ($n = \pm 1, \pm 2$). The constants of integration in (46) are fixed by the condition $\varphi_{n0} = \pi$.

tions. Thus, for $R/l \ll 1$, we have [18,20]:

$$\phi_n(\varphi) \approx \frac{(1 + \operatorname{sgn} \gamma) \pi}{2} + n(\varphi - \varphi_0) + \frac{R^2}{n^2 l^2} \sin[n(\varphi - \varphi_0)]. \quad (\text{A3.1})$$

The self-energy of soliton solutions (A3.1) is

$$F_{sol}(n) \approx \frac{\Phi_0^2 \varepsilon}{2 \mathcal{L}_m} |n|^2 c_1 c_2 \left(1 + \frac{2R^2}{|n|^2 l^2} \right). \quad (\text{A3.2})$$

(Notice that expression (A3.2) clearly illustrates the general features of the self-energy of soliton solutions established in Sec. 4.)

In the opposite limiting case, when $1 \ll R/l < \infty$, asymptotics can be derived only for the single-soliton solutions ($|n|=1$). Fixing the constants of integration by the condition $\varphi_{n0} = \pi$, we get:

$$\phi_{\pm 1}(\varphi) = \frac{(1 + \operatorname{sgn} \gamma) \pi}{2} \pm \left[-\pi + 4 \arctan e^{\frac{R(\varphi - \pi)}{l}} + 8e^{-\frac{2\pi R}{l}} \sinh \frac{R(\varphi - \pi)}{l} + o\left(e^{-\frac{2\pi R}{l}}\right) \right]. \quad (\text{A3.3})$$

The self-energy of these solutions is

$$F_{sol}(\pm 1) = \frac{\Phi_0^2 \varepsilon}{\mathcal{L}_m} \frac{4R}{\pi l} c_1 c_2 \left[1 + o\left(e^{-\frac{2\pi R}{l}}\right) \right]. \quad (\text{A3.4})$$

Solutions (A3.4) approach the well-known[18] exact single-soliton solutions of the static sine-Gordon equation on an infinite interval:

$$\phi_{\pm 1}(\varphi) = \frac{(1 + \operatorname{sgn} \gamma) \pi}{2} \pm \left[-\pi + 4 \arctan e^{\pi x} \right],$$

$$x \equiv \frac{R(\varphi - \pi)}{\pi l} \in (-\infty, +\infty).$$

1. Y. Tanaka, *Phys. Rev. Lett.* **88**, 017002 (2002).
2. H. Bluhm, N.C. Koshnick, M.E. Huber, and K.A. Moler, *Phys. Rev. Lett.* **97**, 237002 (2006); *ibid.* **98**, 209902(E) (2007). It should be noted that the authors "mimicked" two-band superconductivity by using superconducting rings consisting of two parallel, Josephson-coupled aluminium layers. However, in this particular geometrical configuration, the composite system behaves like a genuine two-band superconductor: see the discussion of the Gibbs free-energy functional (8).
3. E. Babaev, *Phys. Rev. Lett.* **89**, 067001 (2002); *Nucl. Phys.* **B686**, 397 (2004).
4. Y. Tanaka, A. Iyo, K. Tokiwa, T. Watanabe, A. Crisan, A. Sundaresan, and A. Terada, *Physica* **C470**, S996 (2010); *ibid.* 1010 (2010).
5. See E. Mertzbacher, *Am. J. Phys.* **30**, 237 (1962) for a clear discussion of this nontrivial condition in quantum physics.
6. The integers n_1 and n_2 are called "topological numbers" or "winding numbers": see, e.g., N.D. Mermin, *Rev. Mod. Phys.* **51**, 591 (1979).
7. M.E. Zhitomirsky and V.H. Dao, *Phys. Rev.* **B69**, 054508 (2004).

8. A. Gurevich and V.M. Vinokur, *Phys. Rev. Lett.* **90**, 047004 (2003); *ibid.* **97**, 137003 (2006).
9. Y.S. Yerin and A.N. Omelyanchouk, *Fiz. Nizk. Temp.* **33**, 538 (2007) [*Low Temp. Phys.* **33** 491 (2007)].
10. Y.S. Yerin, S.V. Kuplevakhsy, and A.N. Omelyanchouk, *Fiz. Nizk. Temp.* **34**, 1131 (2008) [*Low Temp. Phys.* **34**, 891 (2008)].
11. J. Geyer, R.M. Fernandes, V.G. Kogan, and J. Schmalian, *Phys. Rev.* **B82**, 104521 (2010).
12. See S.V. Kuplevakhsy and S.V. Naydenov, *Phys. Rev.* **B56**, 2764 (1997) for a microscopic derivation of functionals of the type (8) in this particular case.
13. The same arguments apply to single-gap superconductors as well: see, e.g., P. G. de Gennes, *Superconductivity of Metals and Alloys Benjamin*, New York (1966).
14. V.L. Ginzburg, *Zh. Eksp. Teor. Fiz.* **42**, 299 (1962).
15. I.N. Askerzade, *Physics-Uspeski* **49**, 1003 (2006).
16. See, e.g., L.D. Landau and E.M. Lifshitz, *Electrodynamics of Continuous Media*, Pergamon Press, Oxford (1968). For reference purposes, we remark that the kinetic inductance is $\mathcal{L}_k = \mathcal{L}_m(1 - 2\varepsilon)/\varepsilon$, as follows from relation (37). Accordingly, the expansion parameter can be expressed as $\varepsilon = \mathcal{L}_m / (\mathcal{L}_k + 2\mathcal{L}_m) \approx \mathcal{L}_m / \mathcal{L}_k \ll 1$.
17. I.V. Krive and A.S. Rozhavsky, *Int. J. Mod. Phys.* **6**, 1255 (1992).
18. S.V. Kuplevakhsy and A.M. Glukhov, *Phys. Rev.* **B73**, 024513 (2006).
19. M. Abramowitz and I.A. Stegun, *Handbook of Mathematical Functions*, Dover, New York (1965).
20. S.V. Kuplevakhsy and A.M. Glukhov, *Phys. Rev.* **B76**, 174515 (2007); *Fiz. Nizk. Temp.* **36**, 1253 (2010) [*Low Temp. Phys.* **36**, 1012 (2010)].
21. R. Jackiw, *Rev. Mod. Phys.* **49**, 681 (1977).
22. E. Babaev, A. Sudbo, and N.W. Ashcroft, *Nature (London)* **431**, 666 (2004).